

## Electronic Supplementary Information

### **High-Performance Flexible Thermoelectric Generator by Control of Electronic Structure of Directly Spun Carbon Nanotube Webs with Various Molecular Dopants**

Cheng Jin An, Young Hun Kang, Hyeonjun Song, Youngjin Jeong, and Song Yun Cho\*

#### **Experimental Section**

*Preparation of CNT Web:* Continuous CNT webs were produced in a furnace from a liquid feedstock consisting of acetone as a carbon source, ferrocene (0.2 wt%) as a catalyst precursor, and thiophene (0.8 wt%) as a promoter. The furnace temperature was maintained at 1473 K, and the carrier H<sub>2</sub> gas was injected at a rate of 1000 sccm. The rate of liquid injection (acetone, ferrocene, and thiophene) was 10 mL/h. The synthesis was conducted by injecting the mixture into a heated reactor under flowing H<sub>2</sub>, as described elsewhere.<sup>1,2</sup> The CNTs were organized into continuous tubular forms, called a CNT sock. The CNT sock was wound onto a winder at the end of the reactor. The CNT web was densified by immersion in dimethyl sulfoxide and drying in an oven at 373 K.<sup>3</sup>

*Preparation of BV Solution and Doping:* The benzyl viologen (BV) solution was prepared via the method described in reference.<sup>4</sup> Briefly, BV (5–40 mg, Sigma–Aldrich) was dissolved into deionized water (10 mL) followed by the addition of toluene (10 mL) to make a bilayer. Sodium borohydride (7.5 g, Sigma–Aldrich) was added to the water/toluene bilayer solution, which was stored for 1 day. The organic layer was then extracted and used for doping. Doping for the CNT web was performed by immersion of the free-standing sheet into the BV solution for 10 h. N<sub>2</sub> gas was then used to remove the residual solvent.

*Experimental Setup for Seebeck Coefficient Measurement:* The Seebeck coefficients of the free-standing CNT webs were measured using a custom system. Dot-shaped Au electrodes were deposited by thermal evaporation on the top of the samples through a shadow mask to minimize

the contact resistance with the probe (Fig. S7a). The distance between the two electrodes was 3 cm, and the diameters of the circular electrodes were 5 mm. The samples were then placed on top of two Peltier plates, and a temperature difference was applied across the sample by applying an electrical current through the two Peltier plates (Fig. S7b). A Keithley 2460 source meter was used to control the temperature of the hot and cold Peltier plates (Fig. S7c). A pair of thermocouples was placed onto the surface of the sample to detect differences in local temperature. The temperature gradient between the electrodes was varied gradually from 1 to 10 K. Meanwhile, a pair of probes was directed toward the previously deposited Au electrodes to measure the TE voltage, which ensured that the measured voltage corresponded precisely to the recorded temperature difference. By varying the temperature difference through the control of the current to the Peltier devices, the TE voltage versus temperature difference was automatically recorded by a Keithley 2182A nano-voltmeter. The Seebeck coefficient was then obtained by analyzing the linear regression slope of the  $\Delta V$ - $\Delta T$  curve.

*Measurements of the Electrical Conductivity:* The electrical conductivity was measured using the standard van der Pauw direct-current four-probe method.<sup>5</sup> All the measurements were conducted at room temperature using a Keithley 195A digital multimeter and Keithley 220 programmable current source. The thicknesses of the films were determined from both cross-sectional scanning electron microscopy (SEM) images and profiles obtained using an alpha-step surface profiler ( $\alpha$ -step DC50, KLA Tencor).

*Measurements of the Thermal Conductivity:* The thermal conductivity  $\kappa$  was calculated using the equation  $\kappa = \alpha\rho C_p$ , where  $\alpha$  is the thermal diffusivity,  $\rho$  is the density calculated based on the measured weight and volume of the webs, and  $C_p$  is the specific heat capacity at constant pressure. The in-plane thermal diffusivity  $\alpha$  of the free-standing webs was measured using a scanning laser heating analyzer (Laser PIT, Ulvac-Riko, Inc.)<sup>6</sup> at 300 K.  $C_p$  was measured using a modulated differential scanning calorimeter (MDSC Q200, TA Instruments). The experimental results of the thermal conductivity measurements of the webs are summarized in

Table S1. The thermal conductivity was measured in the same direction as the Seebeck coefficient measurements.

*Fabrication of the TE Module:* The TE module composed of the BV-doped a-CNT webs and F4TCNQ-doped p-CNT webs as *n*- and *p*-type materials, respectively, was fabricated as follows. Both types of materials were alternatively attached on a flexible plastic substrate via the wet transfer method. Then, the TE webs were electrically connected by Ag paste through dispensing equipment (Musashi Shotmaster 200DS-S, Musashi Engineering, Inc.), followed by sintering at 150 °C on a hot plate for 30 min. The legs of the CNT web, measuring 12 mm in length and 1.5 mm in width, were arranged at intervals of 1.5 mm on a polyethyleneterephthate (PET) substrate (Fig. S6).

*Measurements of Power-generation Characteristics:* The power generation of the TE module was measured using a previously reported custom system.<sup>7</sup> One side of the TE module was heated by applying an electrical current through a hot Peltier plate; the other side was simultaneously cooled to maintain a constant temperature of 20 °C. We set the temperature difference of  $\Delta T = 20$  °C in the in-plane direction between the two sides of the device. The temperature difference of the surfaces of the device was measured by thermocouples. The voltage–current and power output–current curves were measured by varying the load resistance from 0 to 500  $\Omega$ .

*Simulation for Heat Diffusion:* A commercial finite element method (FEM) simulation tool in COMSOL Multiphysics software was used to compare the thermal diffusion behavior of the doped CNT bundle with that of the pristine CNT bundle. The diameter of the CNT bundle and thickness of the molecular dopant were measured to be 26 and 3 nm, respectively. The thermal conductivity of the CNT bundle was measured from the p-CNT web using a scanning laser heating analyzer. The thermal conductivity for the molecular dopant was supposed to be 0.5 W m<sup>-1</sup> K<sup>-1</sup>, which is similar to those of conventional polymers<sup>8</sup> and the thermal conductivity for air was obtained from the material database in the FEM simulation tool. The heat source set as

321 K was positioned at one end of the CNT bundle, and the heat was either radiated to the environment or transferred along the direction of the CNT bundle. The response and intensity of the resulting radiation were closely related to the thermal properties of the CNT web and molecular dopant.

*Characterization of Structures:* The surface morphology was characterized using SEM (SigmaHD, Carl Zeiss). The cross-sectional sample was prepared using the *ex situ* lift-out technique of focused ion beam machining (FB-2100, Hitachi) and imaged using field-emission SEM (SigmaHD, Carl Zeiss). Raman spectra were obtained using high-resolution dispersive Raman spectroscopy (XploRA<sup>TM</sup>PLUS, Horiba Jobin Yvon). UV-photoelectron spectroscopy (UPS) spectra were measured using a base pressure of  $5 \times 10^{-10}$  Torr and He I line ( $h\nu = 21.2$  eV) (Sigma Probe, Thermo VG Scientific).

## Notes and references

- 1 Y.-L. Li, I. A. Kinloch, A. H. Windle, *Science*, 2004, **304**, 276–278.
- 2 X. H. Zhong, Y. L. Li, Y. K. Liu, X. H. Qiao, Y. Feng, J. Liang, J. Jin, L. Zhu, F. Hou, J.-Y. Li, *Adv. Mater.*, 2009, **21**, 1–5.
- 3 K. Liu, Y. Sun, R. Zhou, H. Zhu, J. Wang, L. Liu, K. Jiang, *Nanotechnology*, 2010, **21**, 045708.
- 4 S. M. Kim, J. H. Jang, K. K. Kim, H. K. Park, J. J. Bae, W. J. Yu, I. H. Lee, G. Kim, D. D. Loc, U. J. Kim, E. H. Lee, H. J. Shin, J. Y. Choi, Y. H. Lee, *J. Am. Chem. Soc.*, 2009, **131**, 327-331.
- 5 L. T. Van der Pauw, *Philips Res. Rep.*, 1958, **13**, 1-9.
- 6 L. M. Veca, M. J. Mezziani, W. Wang, X. Wang, F. S. Lu, P. Y. Zhang, Y. Lin, R. Fee, J. W. Connell, Y. P. Sun, *Adv. Mater.*, 2009, **20**, 2088–2092.
- 7 C. T. Hong, Y. H. Kang, J. Ryu, S. Y. Cho, K.-S. Jang, *J. Mater. Chem. A*, 2015, **3**, 21428–21433.

8 H. Chen, V. V. Ginzburg, J. Yang, Y. Yang, W. Liu, Y. Huang, L. Du, B. Chen,  
*Progress in Polymer Science*, 2016, **59**, 41-85.

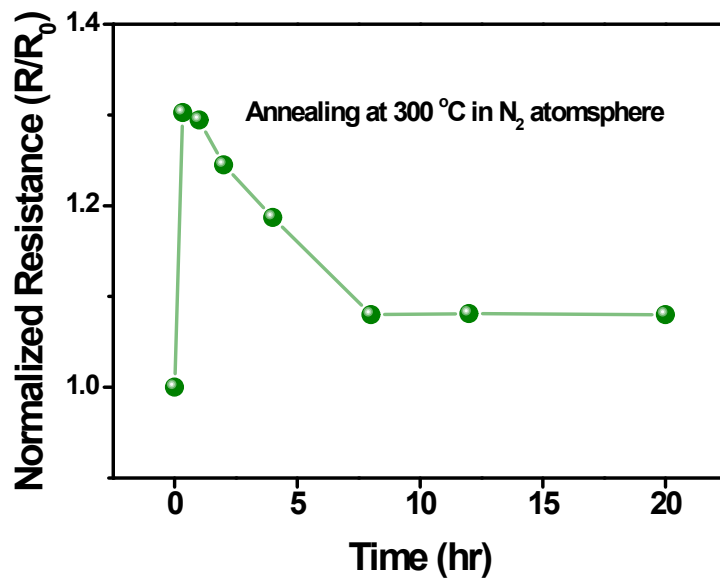


**Fig. S1** Normalized resistance of p-CNT web as a function of annealing time at 300 °C in N<sub>2</sub> atmosphere.

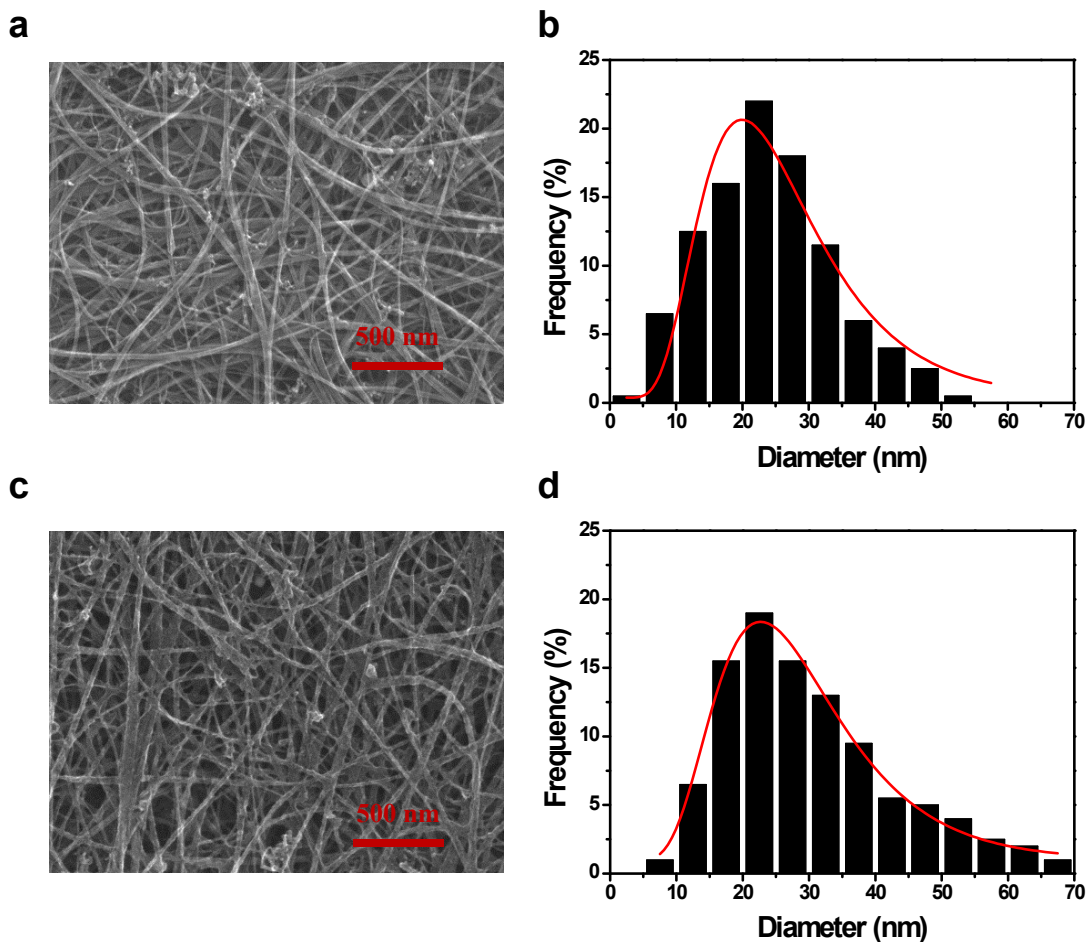


**Fig. S2** (a and c) High-resolution SEM images and (b and d) corresponding bundle size distributions of the p-CNT and BV-doped a-CNT webs, respectively. The distribution of the bundle size was fit using a log-normal distribution, as presented by the red lines. The average bundle diameter was 24.2 nm with a standard deviation of 9.88 nm for the p-CNT web and 30.48 nm with a standard deviation of 13.66 nm for the BV-doped a-CNT web.

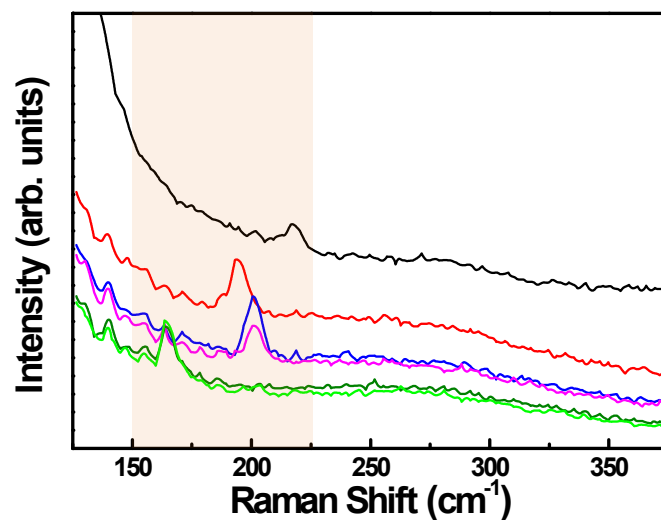


**Fig. S3** Raman spectra of p-CNT web in radical breathing mode region. Single broad peaks in the range from 150 to 225 cm<sup>-1</sup> for the semiconducting portion were observed at six different locations on p-CNT web sample, while peaks corresponding to metallic portion in the range from 225 to 290 cm<sup>-1</sup> were hardly found, probably because the content of metallic-CNT is too low to be detected.

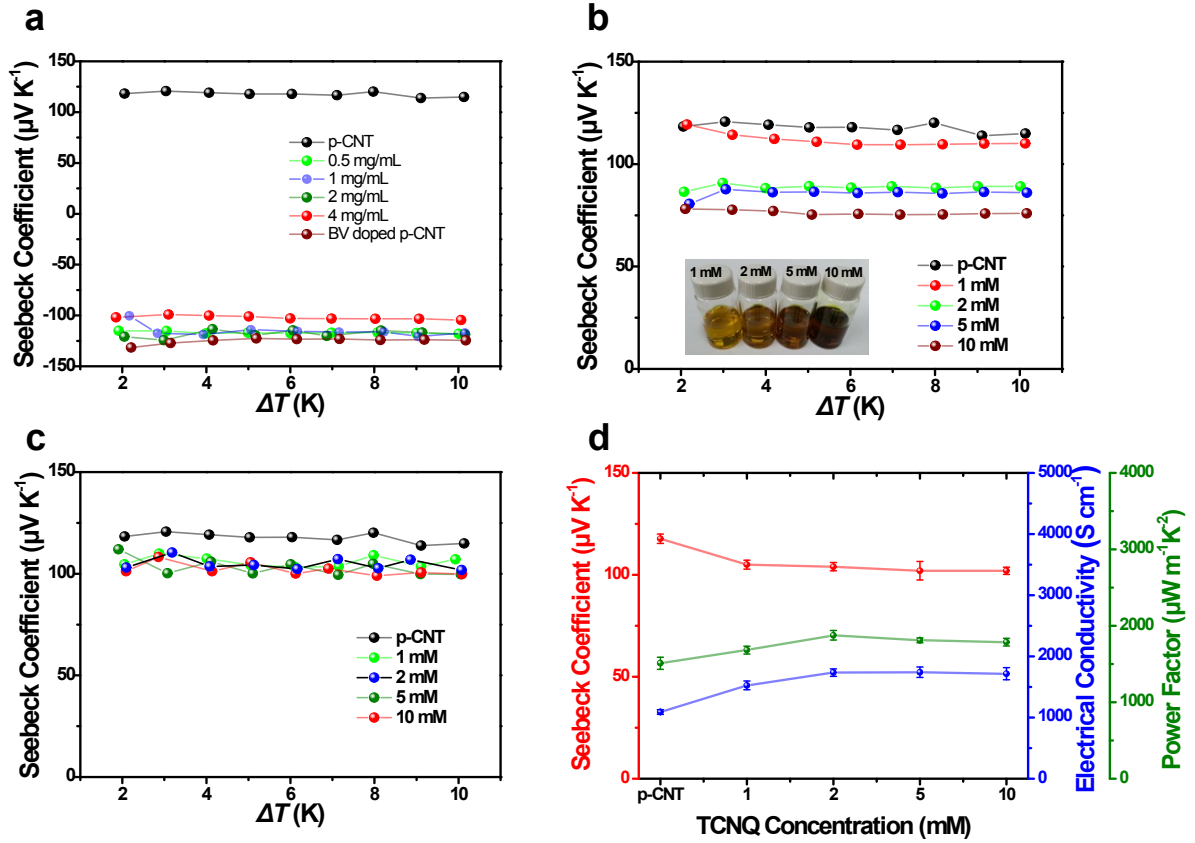


**Fig. S4** Seebeck coefficient vs. temperature for (a) BV-doped a-CNT webs, (b) F4TCNQ-doped p-CNT webs, and (c) TCNQ-doped p-CNT webs as a function of the dopant concentration. The inset presents a photograph of the F4TCNQ dopant solutions with different concentrations. (d) Seebeck coefficient (red filled circles), electrical conductivity (blue filled circles), and corresponding power factor (green filled circles) vs. TCNQ dopant concentration.

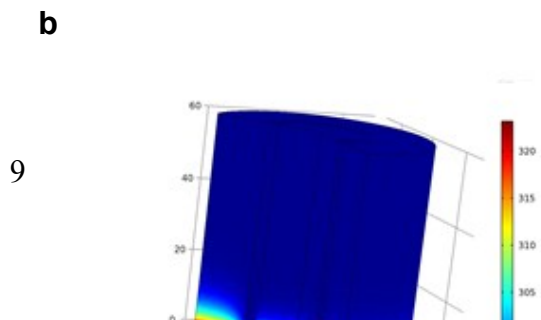
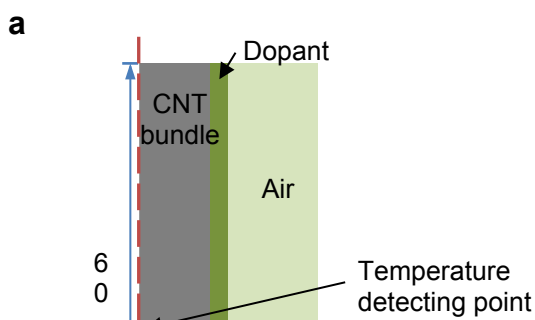


**Fig. S5** Simulation for heat diffusion of doped CNT web: (a) Dimensions of dopant-coated CNT bundle surrounded by air. Heat distribution of dopant-coated CNT bundle (b) before heating and (c) after heating for 0.4 ns. (d) Heat distribution of p-CNT bundle after heating for 0.4 ns. (e) Temperature as a function of heating time at detection point at constant temperature of 323.15 K. (f) Transport mechanisms of phonons (left side) and electrons (right side) within dopant-coated CNT bundle.

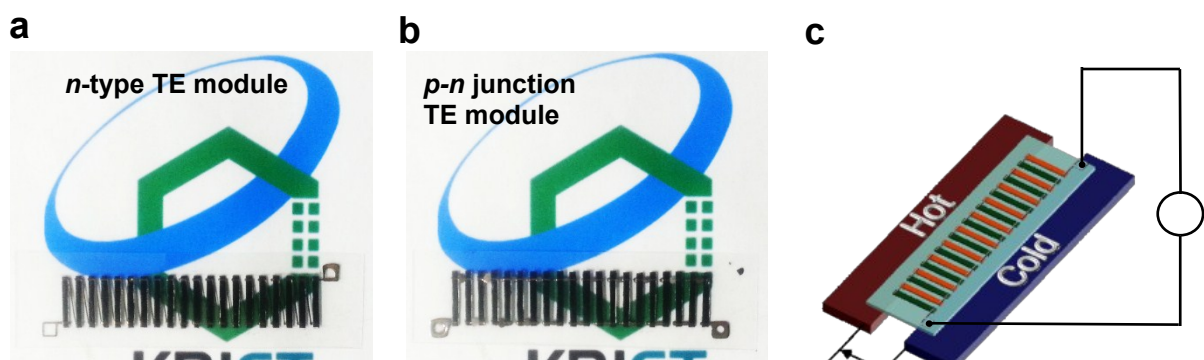


**Fig. S6** Photographs of (a) flexible *n*-type TE module, which is composed of 20 legs of BV-doped a-CNT webs and silver electrodes on a PET substrate and (b) flexible *p*-*n* junction TE module, where the *n*-type legs are alternatively connected with F4TCNQ-doped *p*-type legs. (c) Schematic illustration of the application of the temperature difference of 20 °C between the two sides of the legs with two Peltier plates.

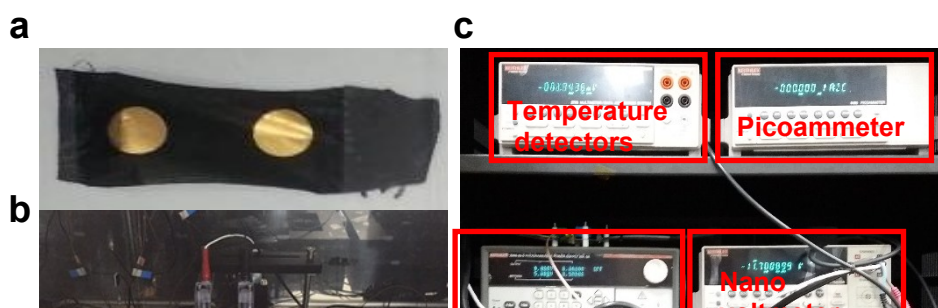


**Fig. S7** (a) Photograph of the sample prepared for the Seebeck coefficient measurement, (b) experimental setup for the Seebeck coefficient measurement, and (c) detectors for temperature and voltage and temperature controller for the Peltier plate.

**Table S1** Thermal conductivity ( $\kappa$ ) and related data for CNT webs at 300 K

CNT web	Thermal diffusivity, $\alpha$	Specific heat capacity, $C_p$	Density, $\rho$ [g cm <sup>-3</sup> ]	Thermal conductivity, $\kappa$
---------	-------------------------------	-------------------------------	---------------------------------------	--------------------------------

	[mm <sup>2</sup> s <sup>-1</sup> ]	[J g <sup>-1</sup> K <sup>-1</sup> ]		[W m <sup>-1</sup> K <sup>-1</sup> ]
p-CNT	20.15 ± 1.2	0.69 ± 0.03	0.41 ± 0.03	5.7 ± 0.2
BV-doped p-CNT web	15.01 ± 0.8	0.78 ± 0.03	0.42 ± 0.03	4.91 ± 0.16
BV-doped a-CNT web	15.31 ± 0.8	0.78 ± 0.04	0.42 ± 0.02	5.01 ± 0.18
F4TCNQ-doped p-CNT web	17.79 ± 0.9	0.79 ± 0.03	0.42 ± 0.02	5.9 ± 0.3